Desalination 439 (2018) 138–146

Contents lists available at ScienceDirect

Desalination

journal homepage: www.elsevier.com/locate/desal

UV radiation pretreatment for reverse osmosis (RO) process in ultrapure water (UPW) production

Yongxun Jin[a,b], Hyunkyung Lee[a], Min Zhan[a], Seungkwan Hong[a,*]

[a] School of Civil, Environmental & Architectural Engineering, Korea University, Seoul 02841, South Korea
[b] Center for Water Resource Cycle Research, Korea Institute of Science and Technology, Seoul 02792, South Korea

GRAPHICAL ABSTRACT

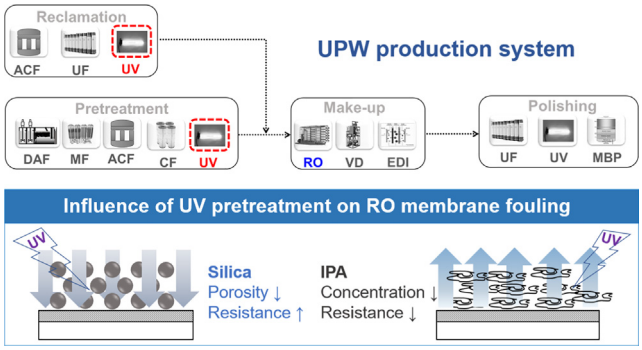

ARTICLE INFO

Keywords:
Ultrapure water (UPW)
Ultraviolet (UV)
Modified fouling index (MFI)
Reverse osmosis (RO)
Membrane fouling

ABSTRACT

In ultrapure water (UPW) production, ultraviolet (UV) radiation is an effective process for reducing microorganisms and organic matter. An increasing trend of reusing the spent UPW further encourages the adoption of UV at the upstream of reverse osmosis (RO) to mitigate membrane fouling and to enhance water quality. In this study, UV technology, both low and medium pressure lamps, was assessed for RO pretreatment in UPW production. The fouling potential of problematic pollutants (e.g., silica and IPA) was evaluated pre and post UV treatment based on fouling index under constant flux mode. We found that the rejection rate of IPA was enhanced up to 80% and thus reduced the organic fouling potential in RO. On the contrary, for inorganic nanoparticle such as silica, a significant increase in fouling potential after UV exposure was observed. Zeta and small angle X-ray scattering analysis implied that this fouling potential transition was derived from silica particle agglomeration under UV radiation. The RO fouling tests corroborated findings from fouling index measurements, showing severe flux decline after UV radiation. This research provides new insight for UPW production design by revealing the influence of UV on inorganic and organic pollutants during the reclamation of spent UPW.

1. Introduction

The significance of ultrapure water (UPW) has been recognized in many advanced high-tech industrial applications, including semiconductors, memory, and LCDs. An extremely pure water is required in large quantities, an important challenge in these industries [1–3]. The UPW production system contains a number of purification technologies that are broadly categorized into three stages: (1) pretreatment to remove suspended solids, (2) make-up to desalt, and (3) polishing to raise water quality sufficiently to meet the production line purpose [4].

* Corresponding author.
E-mail address: skhong21@korea.ac.kr (S. Hong).

https://doi.org/10.1016/j.desal.2018.04.019
Received 30 June 2017; Received in revised form 12 April 2018; Accepted 17 April 2018

Table 1
Specific properties of colloidal silica and isopropanol alcohol (IPA) used in this study.

Foulant	Size	Specific gravity (20 °C)	Viscosity (mPa·s)	Proportion (%)	pH (20 °C)	Supplier
Silica	10–15 nm	1.213	6.5	30.5%	9.5–10.5	SNOWTEX
IPA	MW = 60.1	0.79	1.959	99.7%	7.38	SIGMA ALDRICH

Modern UPW production systems generally include reverse osmosis (RO), which can reliably remove the majority of dissolved ions [4–6].

Although RO is regarded as central to the UPW production system, ultraviolet (UV) radiation is another technology capable of achieving ultra-high purity [4]. In general, UPW plants are reluctant to adopt chemical-based treatment methods since residual chemicals could have deleterious effects on subsequent purification processes. Therefore, UV lamps are often introduced to reduce microorganisms and total organic carbon (TOC). Specifically, low pressure (LP) and medium pressure (MP) lamps are located before or after the RO filtration process [7–11]. An LP lamp that emits a central wavelength of 254 nm is often used for germicidal purposes and an MP lamp is employed to reduce TOC, as it produces hydroxyl radicals by the resonance of 185 nm [12,13].

Some recent studies adopted UV at the upstream of RO to mitigate membrane fouling and to enhance water quality [14,15]. Given the nature of the UV process, UV irradiation works well as an alternative biocide and oxidant. However, its synergetic effects with RO in rejecting inorganics and low molecular weight (LMW) organic matter have not been fully investigated [16]. Since the UPW production system is cumulative, the effects of previous stages on latter stages are significant in achieving the required purity [4].

There is a current trend to reuse spent UPW, which means that the reclamation loop loads more pollutants into the RO process. Though flexible design is required according to specific needs, the reclamation loop often includes microfiltration/ultrafiltration (MF/UF) and UV treatment processes before the RO inlet [17,18]. This trend suggests that the use of UV lamps prior to RO is increasing, necessitating investigation of their chain effect reflecting the water composition of reusable UPW. Regarding reclamation, one problematic matter is silica. Particles with a typical size of 10 nm, so-called "killer particles", must be rejected in microelectronic grade UPW production systems [19]. However, a high concentration of silica particles can be present in the final wafer rinse water from the semiconductor fabrication process [20]. Meanwhile, silica particle control is very important for reusable UPW since they can cause severe scaling as RO is operated under high recovery rates [19,21]. In addition, the LMW organic compound such as isopropanol alcohol (IPA) is another problematic pollutant contained in reusable UPW, since it is widely used as organic solvent in the semiconductor industry, but often difficult to be removed completely by RO [22,23].

Various monitoring tools are employed in UPW production systems, including conductivity meters, TOC meters, and particle counters [24]. The parameters measured by these devices are indicative of the target matter contents. However, to evaluate the role of the RO pretreatment stage, fouling indices can be a useful tool to predict the fouling potential of an RO process by reflecting membrane-specific phenomena. For example, silt density index (SDI) and modified fouling index (MFI) have been widely used in seawater desalination plants [25,26]. We expect that MFI measured under UPW-specified conditions could be applied to assess the fouling potential of small inorganic and organic substances (e.g., silica and IPA) and to provide more precise prediction of RO performance.

The aim of this study was to evaluate the effect of UV treatment on RO performance in a UPW production system. The assessment particularly focused on silica particles and IPA, both of which are problematic in the UPW production system. First, the fouling index was systematically optimized to evaluate the fouling potential of the above pollutants. Next, the change in fouling potential after UV radiation was investigated by measuring the fouling index. Finally, UV treatment as a pretreatment for RO was evaluated via a series of lab-scale RO fouling tests. The primary findings from this study are expected to provide new insight in designing and operating UPW processes in terms of UV application.

2. Material and methods

2.1. Model foulants

In this study, the colloidal silica (SiO_2) particle was used as a model particulate foulant in the fouling simulation experiments. Specifically, particle sizes in the range of 10–15 nm were used (Table 1). The particles were diluted with deionized (DI) water (D7429, Easy Pure RO system, Labscience, Korea) to the concentration of 0.25 mg/L. All silica particles were used after sonication (8510E-DTH, Branson Ultrasonic Co., Danbury, CT, USA) for over 2 min to prevent particle aggregation. The size and the shape of silica particles were further verified using a particle size analyzer (Mastersizer, Malvern Ins., Malvern, United Kingdom).

The model LMW organic matter used in this test was isopropanol alcohol (IPA), frequently used [27] to estimate the removal efficiency of TOC (Table 1). IPA is a volatile organic liquid and has a relatively large surface tension. IPA at the desired concentration was also dissolved in DI water. According to the standard guide for UPW used in industry, the silica and IPA concentrations tested were in the range of 0.25–2 mg/L [28].

2.2. Fouling tests

2.2.1. Fouling index measurements

In this study, the filtration set-up was designed to determine the fouling index, such as SDI, $MFI_{0.45}$, and $MFI\text{-}UF_{flux}$. The testing methods for SDI and $MFI_{0.45}$ followed ASTM standard methods [25,26]. Both indices use MF membrane with a nominal pore size of 0.45 μm and a diameter of 47 mm (active membrane area of 0.0014 m^2) measured under a constant operating pressure of 200 kPa at dead-end mode. Meanwhile, the MFI-UF was also measured with a smaller pore size membrane (10 kDa cut-off), with either constant pressure or constant flux mode [29–31] applied to evaluate the fouling potential of RO feed water (Fig. 1). In constant flux mode, the membrane fouling results in an increase of applied pressure and hence the net driving force can be described by Eq. (1) as follows:

$$\mathrm{TMP} = \mu \bullet R_m \bullet J + \mu \bullet J^2 \bullet I \bullet t \tag{1}$$

where J is the flux ($m^3/m^2/s$) and I is the resistivity (m^{-2}) [32,33]. The resistivity of I can be determined from the slope of the linear region in a plot of transmembrane pressure (TMP) vs. time as illustrated by Eq. 1. Then the $MFI\text{-}UF_{flux}$ at constant flux can be calculated by substituting I value as follows:

$$MFI - UF_{flux} = \frac{\mu \bullet I}{2 \bullet \Delta P \bullet A^2} \tag{2}$$

where ΔP is the applied transmembrane pressure (bar), μ is the viscosity ($N{\cdot}s/m^2$) of the feed water at 20 °C, and A is the surface area (m^2). To keep $MFI\text{-}UF_{flux}$ values comparable with other fouling indices, the $MFI\text{-}UF_{flux}$ is standardized to reference conditions, namely: viscosity at 20 °C (η = 0.001 Ns/m^2), pressure of 2 bar (ΔP_0), and surface area of a 10 kDa

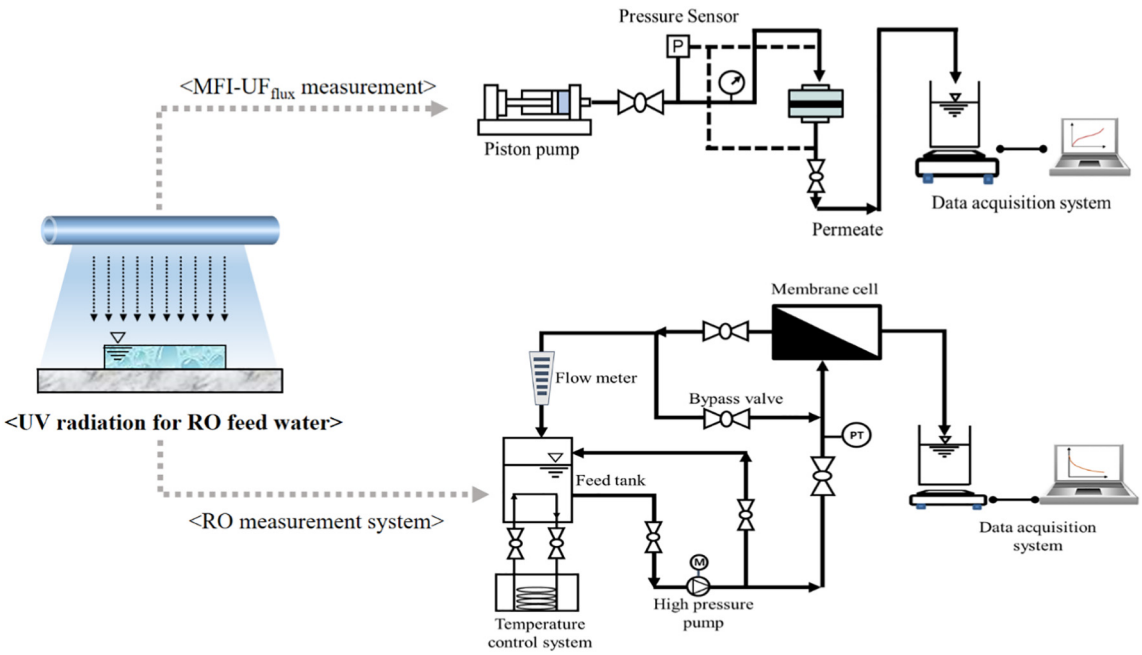

Fig. 1. Schematic diagram of lab-scale MFI-UF_{flux} measurement and RO membrane filtration systems. In the fouling index measurement, the MFI-UF_{flux} was measured with a 10 kDa UF membrane by employing a piston pump in a dead-end flow system. In the RO fouling test, the RO experiments were performed using flat-sheet RO membranes with crossflow filtration at an applied pressure of 20 bar. The concentrate water was recycled back to the feed tank after passing through the membrane cell.

tight UF membrane ($A_0 = 3.8 \times 10^{-4}\,m^2$) [32]. The MFI-$UF_{flux}$ measured in constant flux mode, typically at 100 LMH, often results in different rates of cake compression. Data analysis was performed by SPSS (Statistical Package for the Social Science, IBM SPSS Statistics, Ver. 21.0) software. The regression of fouling test results was plotted by using SigmaPlot (Systat software, Ver 12.5). The relationship between the foulant concentrations and the fouling index (SDI, $MFI_{0.45}$, and MFI-UF_{flux}) was assessed with the concentrations and the fouling index as the dependent and independent variables, respectively.

2.2.2. RO fouling test

Laboratory-scale RO fouling experiments were performed using commercial RO membranes (RE8040-BR, Toray) under cross-flow filtration mode at an applied pressure of 20 bar. This crossflow-flat filtration system was configured using the membrane cell, a high-pressure pump, stirrer, feed reservoir, chiller, and data acquisition system (Fig. 1). The feed water was held in a 4-L reservoir and fed to the membrane cell by high-pressure pump. The initial flux and cross-flow velocity were adjusted to 10 μm/s and 8.5 cm/s, respectively. The effective membrane surface area was $2.0 \times 10^{-3}\,m^2$. Operating parameters such as filtrate flux, crossflow velocity, and pressure were carefully controlled by manipulation of the back-pressure regulator and bypass valve. Finally, the correlation of the measured fouling index values and the flux decline rate (FDR) was established to verify the fouling index values with respect to the experimental RO data [34,35].

The FDR was defined as follows:

$$\Phi = -\frac{1}{J_0^2} tg\theta|_{t=0} = -\frac{1}{J_0^2}\frac{dJ}{dt}\bigg|_{t=0} \tag{3}$$

$$J(t) = \frac{J_0}{\sqrt{1 + 2\Phi J_0 t}} \tag{4}$$

where Φ is the FDR, J_0 ($m^3\,m^{-2}\,s^{-1}$) is the initial flux, t is the filtration time (s), and $tg\theta|_{t=0}$ is the slope of the flux decline curve at $t = 0$. FDRs were calculated by non-linear fitting of the filtration data using the model equations above. In this study, we received the flux data from the electric balance once per minute and calculated the dJ/dt term from an average across the initial 30 min.

2.3. Characteristics of UV sterilizer and reducer

Two types of UV lamps (LP and MP) were used in this experiment since these are the most popular lamp systems currently in use. There is an intrinsic difference between LP and MP lamps; while the wavelength spectrum of LP lamps is concentrated around 254 nm, MP lamp covers a broader spectrum, including 185 nm. Moreover, MP lamps hold much higher output than LP lamps; the light intensity of LP and MP lamps used here were 3.5 mW/cm^2 and 55 mW/cm^2, respectively. Although the MP lamp drives much higher energy in same contact time compared to the LP lamp, we set identical radiation times, as contact time is determined by flow rate, considering the actual operating conditions in a water treatment plant.

The LP lamp (HANSUNG, 105 W), MP lamp (HANSUNG, 7200 W), and a synthetic quartz sleeve (4.5 cm diameter × 24 cm length) were installed in the center of the UV reactor. The distance from the inner wall of the photoreactor to the external wall of the quartz tube was 88 mm. The feed water (i.e., silica and IPA suspension) was continuously supplied to the reactor in circulation by a speed-gear pump (Cole-Parmer, USA) in a closed loop. In the circulation test, the feed flow velocity was set at 0.37 m/s, and the temperature to 25 ± 0.5 °C. The total experimental time varied from 1 to 30 min.

2.4. Foulant analysis

Zeta potential analysis is a measurement of the electric double layer produced by surrounding ions in solution that has been widely used to interpret the agglomeration or disaggregation of colloidal dispersions [36,37]. The change in zeta size and zeta potential was measured before and after UV exposure with a Zetasizer NanoZS (Malvern Instruments, UK). The instrument calculated the zeta potential following the Smoluchowski equation from the measurement of electrophoretic mobility [37] .

$$\zeta = \frac{U\eta}{\varepsilon} \quad (5)$$

where ζ is zeta potential, U electrophoretic mobility, η medium viscosity, and ε is a dielectric constant.

To investigate the overall sizes of radiated silica particles, small angle X-ray scattering (SAXS) was employed by monitoring the R_g value. The SAXS (SAXSess, Anton-Paar) is a structural method applicable to native particles in solution, and it is particularly suitable for smaller structured systems. For monodisperse systems containing randomly oriented particles with identical structures, the isotropic SAXS intensity is proportional to the single particle scattering averaged over all orientations.

3. Results and discussion

This section is comprised of three parts. First, an appropriate fouling index was determined to evaluate the fouling potential in a UPW pretreatment process. Second, the fouling index was applied to illustrate the effect of UV radiation as an RO pretreatment. Finally, an RO fouling test was conducted to verify the effect of UV radiation on RO performance. In particular, inorganic fouling mechanisms related to UV treatment were highlighted in this research.

3.1. Determining fouling potential of feed water in UPW production system

3.1.1. Deficiency of ASTM fouling indices for the UPW-grade water

According to an ASTM statement, SDI and $MFI_{0.45}$ were developed to indicate the fouling potential of RO feed water, primarily due to particulate matter [16,24]. As such, SDI and $MFI_{0.45}$ were first measured to evaluate the fouling potential of RO feed water. To determine both indices, the feed water was filtered at constant pressure through a 0.45-μm MF membrane in dead-end flow. Meanwhile, the rejection rate of filtration tests was also measured as a parameter of foulant removal.

As shown in Fig. 2, SDI and $MFI_{0.45}$ values increased with increasing foulant concentration, although all these values are very low, indicating no or small fouling potentials. According to the regression analysis from the direct proportion of fouling index and concentration, the higher R^2 value of $MFI_{0.45}$ than SDI implies that $MFI_{0.45}$ may predict fouling potential more accurately [29,38]. However, the reliability of the fouling index suffered greatly from low removal by the MF membrane (rejection rate < 10%), which does not simulate the true fouling potential in an RO process. Therefore, tighter membrane pore size was demanded, such as MFI-UF, in order to evaluate the fouling potential of silica and IPA more precisely.

3.1.2. Applicability of MFI-UF$_{flux}$ in UPW pretreatment process

The adaptation of SDI and $MFI_{0.45}$ showed limitations for application in a UPW production system since the 0.45-μm membrane could not fully reflect the influence of colloidal particles that should necessarily be rejected. Therefore, MFI-UF_{flux} measured with a 10 kDa cut-off membrane, the equivalent size of 3.5 nm pore size [39], was applied to evaluate the fouling potential derived from 10 nm silica used in this study. By producing higher silica rejection rates, a more precise simulation of RO performance was expected.

Fig. 3 presents the fouling potential of silica and IPA measured with MFI-UF; both MFI-UF_{flux} and MFI-UF_{pres} showed high linearity with R^2 of 0.98 (significant level $p < 0.05$). Moreover, the overall rejection rate increased significantly in comparison to $MFI_{0.45}$; the rejection rate of silica was around 80% (Fig. 3a) and IPA was around 40% (Fig. 3b). One interesting observation was that MFI-UF_{flux} achieved a higher rejection rate than MFI-UF_{pres}. This can be understood as a result of continuously increased TMP in constant flux filtration mode; the accumulated foulant on the membrane surface could restrict the permeation of entering foulants that are contained in the feed water while maintaining the designated water flux. However, in the case of constant-pressure filtration mode, the flux decreased over time and thus the second membrane effect derived by foulants could be weakened. Consequently, the rate of cake formation and the cake layer characteristics became different, yielding different MFI-UF values.

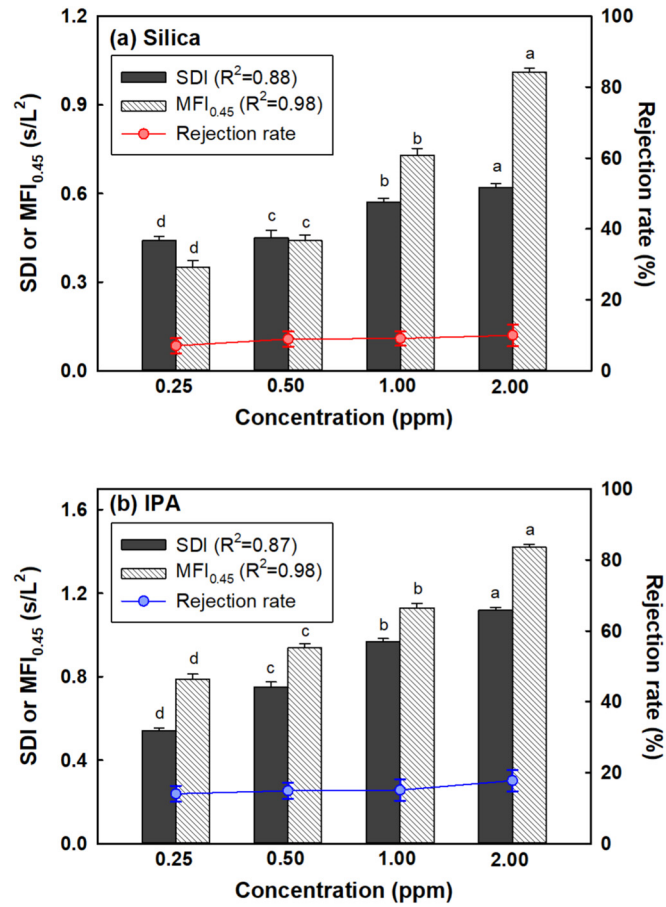

Fig. 2. Comparison of fouling indices (SDI and $MFI_{0.45}$) and rejection rate under the presence of silica and IPA. (a) Standard fouling index (SDI and $MFI_{0.45}$) and rejection rate as silica concentration increases. (b) Standard fouling index (SDI and $MFI_{0.45}$) and rejection rate as IPA concentration increases. The feed suspension used was adjusted from 0.25 to 2 ppm. Experimental conditions: 0.45 μm UF membrane, applied pressure: 2 bar. Different letters indicate significant differences among treatments. Multiple comparisons of means were performed using Tukey's test at the 0.05 significance level.

Finally, owing to its higher rejection rate as well as simulation of RO practice, the MFI-UF_{flux} was selected and correlated with RO performance. By employing the slope of the flux decline period, the FDR was determined for each fouling test. Fig. 4 clearly shows that the MFI-UF_{flux} is directly proportional to the FDR of RO in both silica and IPA suspension, implying an actual fouling potential.

3.2. Investigating the influence of UV radiation on fouling potential of RO feed water

UV technology has been often applied in downstream of RO for TOC reduction or disinfection in UPW systems [4]. Recently, an industrial trend to reuse the spent UPW further increases the use of UV treatment to improve water quality prior to RO [17,18]. Table 2 provides a summary of UV applications in industrial water production in terms of UV type, purpose, installation location to RO, and feed water characteristics.

To assess the effect of UV pretreatment on RO performance in a UPW production system, we adopted MFI-UF_{flux} to evaluate the change in fouling potential before and after UV treatment. Fig. 5 shows the

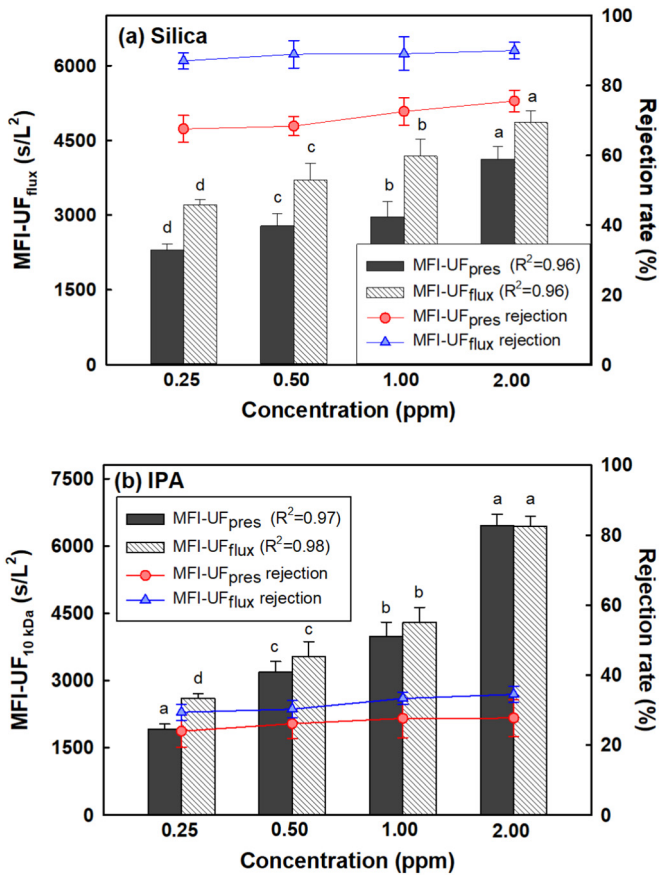

Fig. 3. Fouling potential evaluation in constant flux and pressure filtration modes: (a) MFI-UF$_{flux}$ values and rejection rate as silica concentration increases. (b) MFI-UF$_{pres}$ values and rejection rate as IPA concentration increases. Experimental conditions: 10 kDa UF membrane, applied pressure: 2 bar (MFI-UF$_{pres}$), applied flux: 100 LMH (MFI-UF$_{flux}$), the feed water suspension used was adjusted from 0.25 to 2 ppm. Different letters indicate significant differences among treatments. Multiple comparisons of means were performed using Tukey's test at the 0.05 significance level.

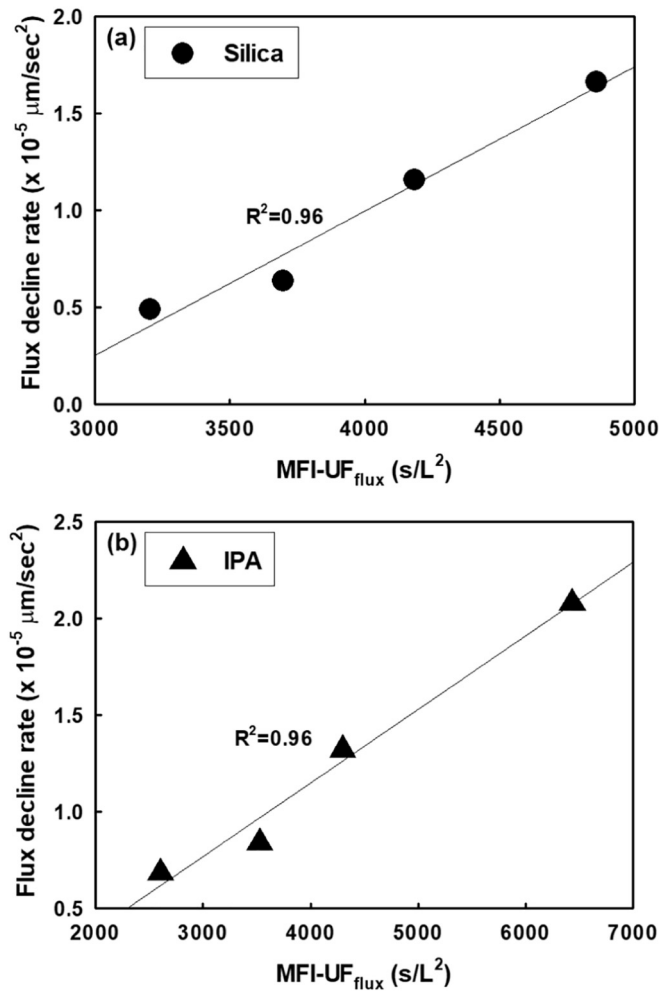

Fig. 4. Relationship between flux decline rate (FDR) and the MFI-UF$_{flux}$ with respect to silica and IPA foulants. Experimental conditions: silica concentration = 0.25–2 ppm, IPA concentration = 0.25–2 ppm.

influence of UV radiation on the fouling potential of silica and IPA. In case of the silica, the MFI-UF$_{flux}$ increased after UV treatment, and the MP lamp resulted in more severe change compared to the LP lamp (Fig. 5a). This result implies that delivery of UV energy can increase the fouling potential of silica particles, and that such transition can be wavelength-dependent.

IPA showed an opposite trend. The MFI-UF$_{flux}$ showed a decrease after both LP and MP treatment (Fig. 5b). This observation can be explained as a result from the decomposition of organic compounds by UV lamp systems [7,40]. Particularly noteworthy was that the decrease was not only observed with the MP lamp but also with the LP lamp, meaning that the < 200 nm wavelength could also decompose IPA, though it was much weaker than the MP lamp.

To clarify whether the transition was wavelength-dependent or dose-dependent, a comparative test of the two lamp systems was performed under UV dose normalization. Since complete light profile unification was impossible due to the inborn characteristics of the lamps, adjusting the radiation time was logically chosen as the optimum approaches for dose normalization. We set the radiation time of the LP system to 18, 54, and 90 min and the MP lamp times to 1, 3, and 5 min based on intensity value. Moreover, this experiment was conducted as a batch test without circulation to eliminate uncontrolled variables.

Table 3 shows the fouling potential of silica suspension after UV treatment; a similar rate of increase was observed for both lamp systems. Though the discrepancy was still present showing higher values under MP lamp treatment, the difference was < 10% of the total value. Therefore, we conclude that UV dose is a dominant factor in controlling the rise of silica fouling potential. In addition, we observed much higher MFI-UF$_{flux}$ under batch test mode compared to circulation test mode (Fig. 5a), where the UV energy is delivered in a constant manner. This result also supports that total UV dose controls the increase in fouling potential. This implies that the UV spectrum does not significantly participate in raising silica fouling potential, yielding similar results from both lamp systems. However, considering practical applications, the negative effect derived from the MP lamp is more significant, since it delivers much higher energy in the same contact time compared to the LP lamp.

To gain a better understanding of such mechanism, SAXS analysis was conducted, which is a reliable tool to determine particle size distribution [27,41]. After UV treatment, the average particle size increased from 9.01 nm to 9.56 nm, although this change is small. Moreover, the zeta size increased even more with decreasing zeta potential according to UV as presented in Fig. 6. These results indicate that UV energy reduced the zeta potential of silica, hence causing the aggregation of silica particles. Such phenomenon was more clearly observed with the MP lamp, as it delivers 18 times more energy than the LP lamp. The overall results suggest that UV radiation as an RO pretreatment holds the risk of inorganic fouling, although it is beneficial to minimize bio- and organic fouling.

Table 2
Overview of UV application in industrial water production system with a focus on RO process.

Type of UV	Feed water	Target process	Location	Purpose	Ref.
Low-pressure lamp	Groundwater	NF/RO process	Before RO	Disinfection	[14]
	Bacteria source water	UPW process	Before RO		[15]
	Bacteria source water	UPW process	Before RO		[7]
	Bactericide water	UPW process	Before RO		[11]
	Wastewater	UPW process	After RO		[18]
	Municipally treated water	UPW process	After RO		[24]
Medium-pressure lamp	Tap water	UPW process	After RO	TOC reduction	[10]
	Synthetic wastewater	UPW process	After RO		[1]
	RO permeate water	UPW process	After RO		[9]
	Tap water	UPW process	After RO		[8]

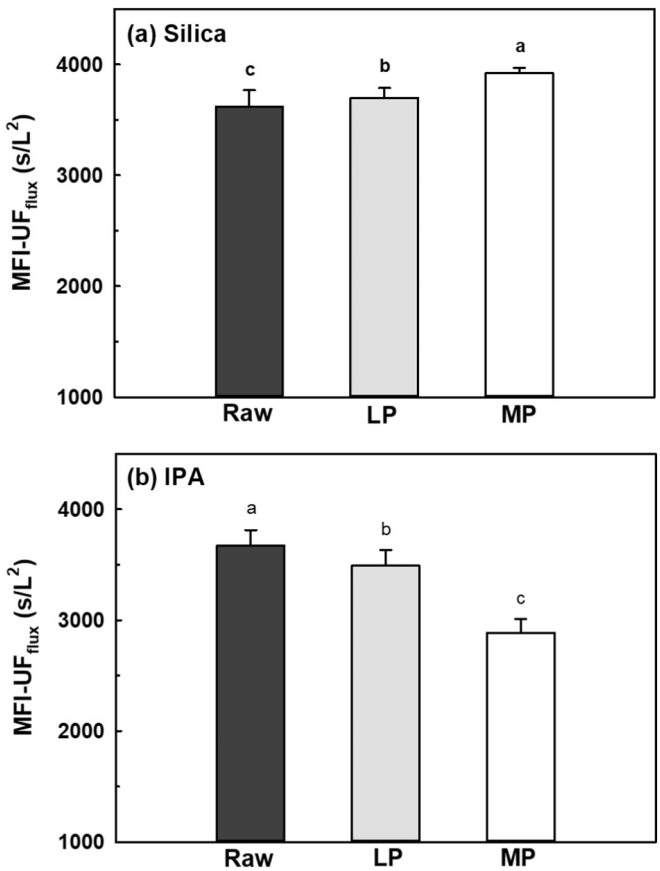

Fig. 5. Fouling index measurements performed under low- and medium-pressure lamp exposure. The fouling tests were conducted using silica and IPA foulants. (a) MFI-UF$_{flux}$ values of silica, experimental conditions: silica 0.5 ppm, UV radiation 30 min; (b) MFI-UF$_{flux}$ values of IPA, experimental conditions: IPA 2 ppm, UV radiation 30 min. in circulation condition. Different letters indicate significant differences among treatments. Multiple comparisons of means were performed using Tukey's test at the 0.05 significance level.

Table 3
Comparison of LP and MP irradiation on the fouling potential of silica particles.

		LP	MP
Fouling potential MFI-UF$_{flux}$ (s/L^2)	Dose 1 (3300 mJ/cm^2)	2752.87 ± 402.32	3043.72 ± 344.28
	Dose 2 (9900 mJ/cm^2)	4372.07 ± 274.30	4587.35 ± 220.95
	Dose 3 (16,500 mJ/cm^2)	5357.96 ± 227.35	6039.46 ± 342.17

Note: the UV dose experiments were conducted in a batch type without circulation to investigate only the variation of particle size distribution.

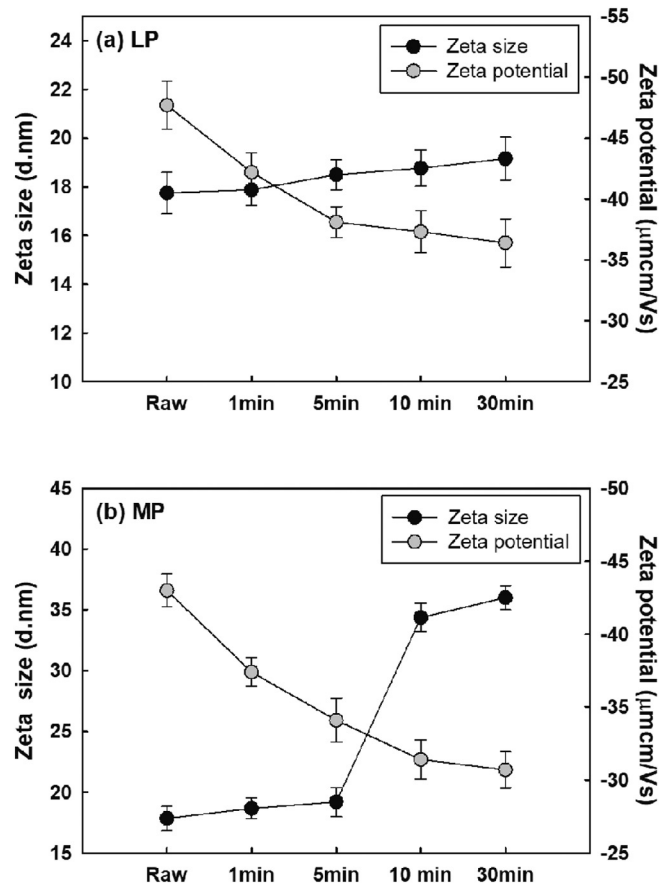

Fig. 6. Variation of zeta size and zeta potential of IPA and silica according to UV. (a) Changes in zeta size and zeta potential under low-pressure lamp (LP), and (b) under medium pressure lamp (MP). Experimental conditions: IPA = 2 ppm, silica = 0.5 ppm.

3.3. Assessment of UV radiation as a pretreatment of RO process

To verify the effect of UV radiation on RO performance, bench-scale RO tests were conducted, and RO performance was evaluated in terms of water permeability and rejection rates. Then, the feasibility of UV radiation was assessed to improve RO performance in UPW treatment.

3.3.1. Validation of UV effect on RO performance

Fig. 7 presents the RO flux decline rates after UV treatment. The RO flux decline with silica increased after UV radiation, and the MP lamp caused more severe deterioration (Fig. 7a). This trend agrees well with the observation in the Section 3.2, that UV drives aggregation among colloidal particles, possibly resulting in decrement of cake layer porosity.

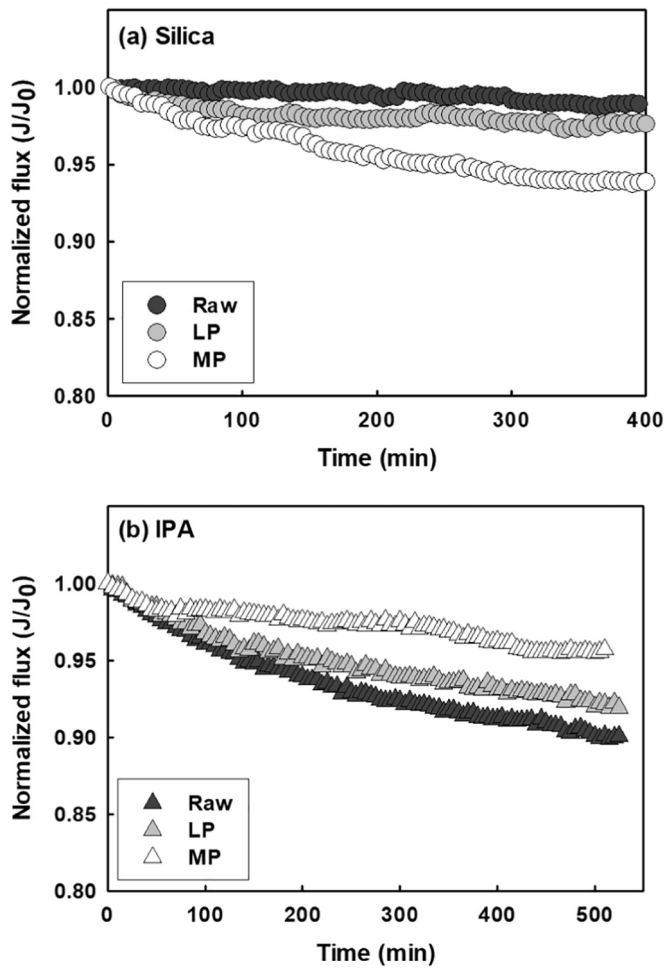

Fig. 7. RO filtration tests performed using silica and IPA pollutants under UV exposure conditions: (a) normalized flux decline for synthetic silica and radiated; (b) normalized flux decline for synthetic IPA and radiated by LP and MP lamps. The compaction for each RO process was conducted over 12 h, and the RO feed water radiation time was kept constant at 30 min.

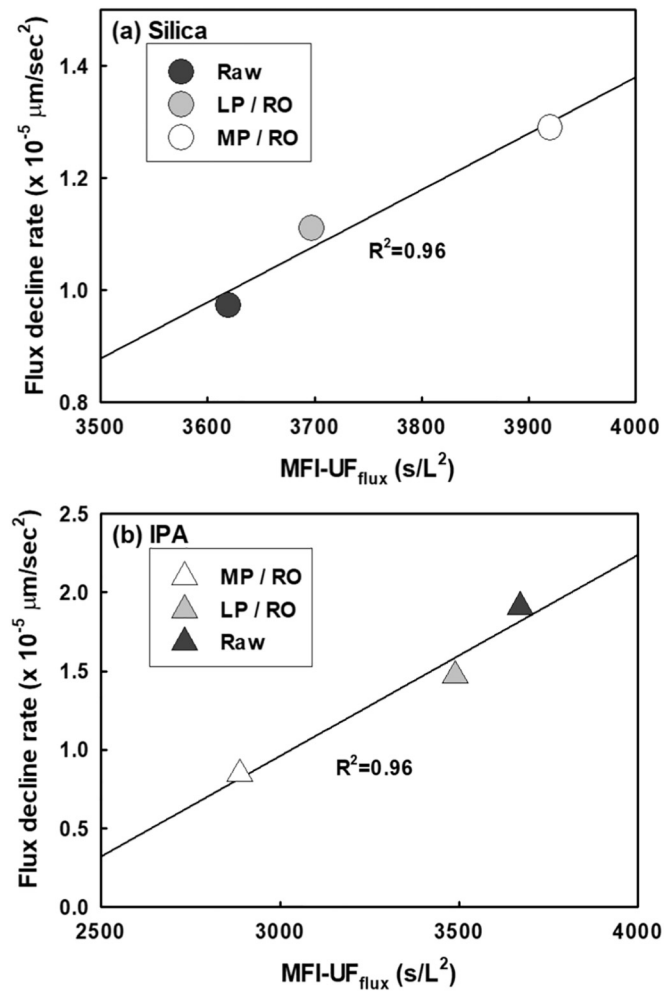

Fig. 8. Relationship between flux decline rate (FDR) and MFI-UF_{flux}: (a) IPA and (b) silica. Experimental conditions: silica concentration = 0.5 ppm, IPA concentration = 2 ppm. The radiation time by both low- and medium-pressure lamps was 30 min.

In addition, RO performance degradation might be explained further based on the characteristics of cross-flow mode. Different from dead-end mode that all of particles in feedwater moves toward the membrane vertically, particles move parallel to the membrane surface in cross-flow mode and consequently only a fraction of particles are deposited on the membrane surface. According to the transport mechanism of small colloids, the deposition of particle increases with increment of particle size when it is in the range of < 100 nm [42]. This means the mass of deposited colloids on membrane surface could be increased due to particle aggregation after UV treatment [42,43]. Furthermore, the transition of silica suspension from monodisperse to polydisperse states could be another reason, therefore the cake porosity may be further reduced by filling up small particles between large aggregates. In the case of IPA, on the other hand, the UV treatment resulted in significantly improved water flux (Fig. 7b). This result manifested decreased organic fouling after UV radiation. Furthermore, the MP lamp resulted in more improvement than the LP lamp, which corresponds to the results of MFI-UF_{flux} measurements.

The effect of UV was further confirmed by plotting the FDR and MFI-UF_{flux} (Fig. 8). As the MFI-UF_{flux} increased, the FDR also increased with both IPA and silica suspensions. Specifically, the lowest MFI-UF_{flux} value among IPA suspensions was obtained after MP lamp treatment, whereas higher FDR resulted with the silica suspensions. This result suggests that UV pretreatment is effective in reducing organic fouling by decomposing organic molecules, but has an adverse effect on inorganic foulants.

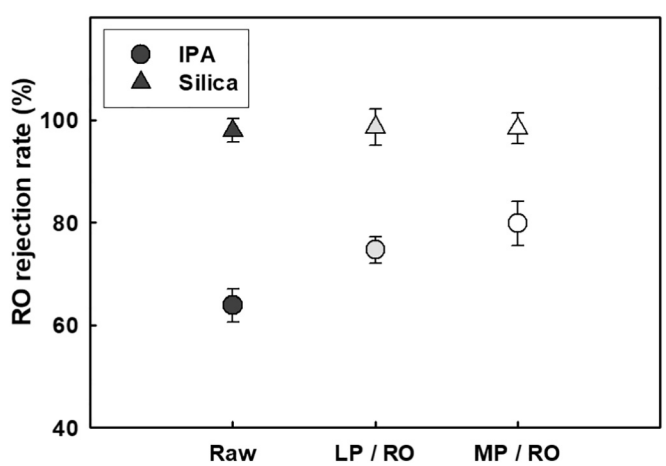

Fig. 9. RO rejection rates of silica and IPA foulants. The raw water and UV-radiated waters by low- and medium-pressure lamps are compared, respectively.

The rejection rate, on the other hand, was maintained (silica) or improved (IPA) after UV radiation (Fig. 9). Specifically, IPA rejection was enhanced after UV pretreatment, owing to the synergetic effects of

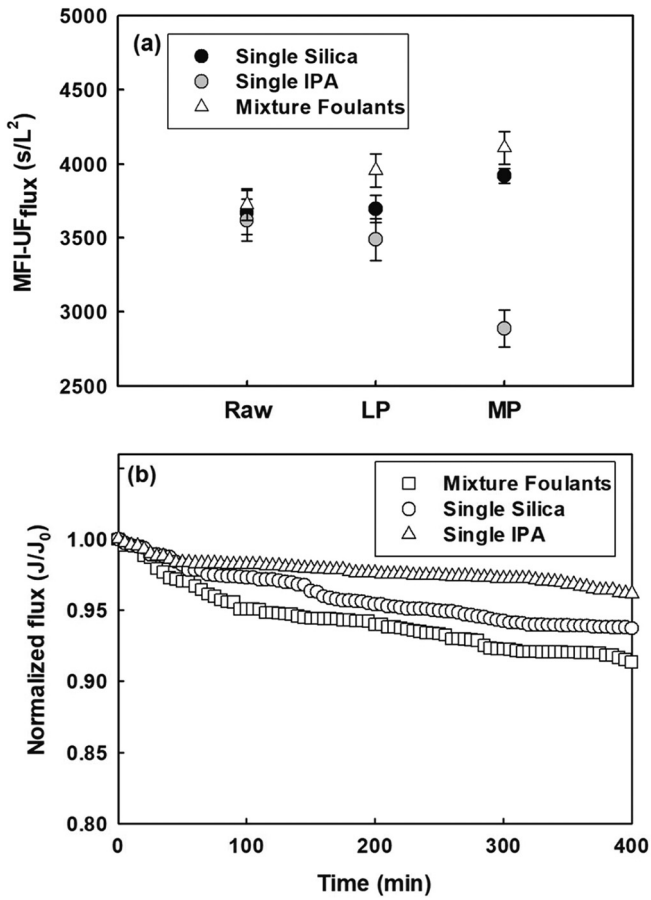

Fig. 10. MFI-UF_{flux} and RO filtration tests performed using a single foulant (silica or IPA) and a mixture of silica (0.5 ppm) and IPA (2 ppm). (a) MFI-UF_{flux} values for silica and IPA were measured under LP and MP lamps, (b) normalized flux decline with single foulants and a mixture of IPA and silica foulants by medium-pressure lamp. The compaction for each RO process was conducted over 12 h.

UV and RO [18]. UV pretreatment reduced IPA loading to RO and thus achieved higher water quality after the RO process. On the contrary, regardless of the water flux decline, there was no significant change in the silica rejection rate (> 98%), and RO fouling was accelerated.

3.3.2. Effect of the combined foulants on RO performance after UV radiation

In these experiments, silica (0.5 ppm) and IPA (2 ppm) were combined and investigated. Compared with the case of a single foulant (either silica or IPA), the fouling potential of the foulant mixture was greater than the individual fouling potential values (Fig. 10a). Although UV irradiation may cause IPA degradation, our results suggest that the inter-particle voids among the silica particle became blocked by organics, thus making the cake layer less porous, and resulting in a higher MFI-UF_{flux} value.

The normalized flux decline in Fig. 10b also confirmed this speculation, comparing UV radiance on silica alone, IPA alone, and their mixtures. Beyond a certain IPA load, increasing flux decline was clearly observed. Moreover, the synergetic effect between the foulants would instill fouling layer with low porosity, resulting in greater resistance. The overall findings from our study suggest that UV pretreatment used for biofouling control in RO may also carry the risk of enhancing inorganic fouling in RO. Thus, UV pretreatment should be designed more carefully, by considering all foulant behaviors, for more effective RO fouling control in UPW treatment. This is especially true given the increasing practice of reclamation of spent UPW.

4. Conclusions

We systematically evaluated UV radiation as a pretreatment for RO, considering the trend to reuse UPW, which means that the reclamation loop loads more pollutants onto the RO process. Using an optimized fouling index to simulate fouling in RO, the effect of UV pretreatment was first assessed in terms of fouling by inorganic and organic residuals in spent UPW. The existing fouling indices for RO from ASTM (i.e., SDI and $MFI_{0.45}$) showed limitations when applied in a UPW system. Thus, MFI-UF_{flux} employing a 10 kDa membrane, measured in constant flux mode, showed higher rejection rates and a more closely simulated RO flux decline.

Although UV radiation is a proven technology to improve water quality in UPW, its effect on RO fouling can be more complex, and thus should be assessed by considering the foulant characteristics in UPW production. UV lamp treatment can cause a negative effect on silica fouling potential over 10%, as MP lamps deliver much higher energy in same contact time than LP lamps. In contrary, the MP lamp caused a more significant decrease in fouling potential, since it decomposes organic compounds by producing hydroxyl radicals.

The approach from this study also showed promise for membrane-specific parameters (e.g., modified fouling index) to evaluate the suitability of UV lamps in a pretreatment stage. This study contributes not only for the proper application of UV treatment, but also for the design of effective UPW pretreatment systems.

Acknowledgements

This research was supported by a grant from Technology Innovation Program (10052814, Technology development of ultra-pure water process for semiconductor level industrial water and localization for 4 kinds of consumable material) funded by the Ministry of Trade, Industry and Energy, South Korea.

References

[1] J. Choi, J.-O. Kim, J. Chung, Removal of isopropyl alcohol and methanol in ultrapure water production system using a 185 nm ultraviolet and ion exchange system, Chemosphere 156 (2016) 341–346.
[2] J. Wood, J. Gifford, J. Arba, M. Shaw, Production of ultrapure water by continuous electrodeionization, Desalination 250 (2010) 973–976.
[3] T.S. Light, S. Licht, A.C. Bevilacqua, K.R. Morash, The fundamental conductivity and resistivity of water, Electrochem. Solid-State Lett. 8 (2005) E16–E19.
[4] H. Lee, Y. Jin, S. Hong, Recent transitions in ultrapure water (UPW) technology: rising role of reverse osmosis (RO), Desalination 399 (2016) 185–197.
[5] E.M. Vrijenhoek, S. Hong, M. Elimelech, Influence of membrane surface properties on initial rate of colloidal fouling of reverse osmosis and nanofiltration membranes, J. Membr. Sci. 188 (2001) 115–128.
[6] M. Ando; S. Ishihara; Method of multi-stage reverse osmosis treatment, United States patent US 102 (2004) 1–8.
[7] W.V. Collentro, A novel approach to control microbial fouling of reverse osmosis elements, Ultrapure Water J. (2014) 27–34.
[8] H.Y. S. Otani, Y. Harada, T. Fujii, S. Suhara, K. Suyama, Ultraviolet oxidation device, ultrapure water production device using same, ultraviolet oxidation method, and ultrapure water production method, Google Patents, (2013).
[9] V. Fedorenko, Ultrapure water production by continuous electrodeionization method: technology and economy, Pharm. Chem. J. 38 (2004) 35–40.
[10] R. Wen, G. Meng, Method for removing organic matter from super-pure water by 185 nano ultraviolet light and film de-airing combination, Google Patents, (2003).
[11] Y.N. M. Abe, System for producing ultra-pure water, Google Patents, (2001).
[12] W. Han, P. Zhang, W. Zhu, J. Yin, L. Li, Photocatalysis of p-chlorobenzoic acid in aqueous solution under irradiation of 254 nm and 185 nm UV light, Water Res. 38 (2004) 4197–4203.
[13] D. Cassan, B. Mercier, F. Castex, A. Rambaud, Effects of medium-pressure UV lamps radiation on water quality in a chlorinated indoor swimming pool, Chemosphere 62 (2006) 1507–1513.
[14] W. Song, V. Ravindran, B.E. Koel, M. Pirbazari, Nanofiltration of natural organic matter with H_2O_2/UV pretreatment: fouling mitigation and membrane surface characterization, J. Membr. Sci. 241 (2004) 143–160.
[15] W.V. Collentro, Production of EP water for injection - a technical overview, Ultrapure Water J. (2015) 31–36.
[16] Y. Rozenberg, Method for preventing biofouling on surfaces using ultraviolet pretreatment, in, Google Patents, 2010.
[17] R. Sheikholeslami, I.S. Al-Mutaz, T. Koo, A. Young, Pretreatment and the effect of cations and anions on prevention of silica fouling, Desalination 139 (2001) 83–95.

[18] M. Wu, D. Sun, J.H. Tay, Process-to-process recycling of high-purity water from semiconductor wafer backgrinding wastes, Resour. Conserv. Recycl. 41 (2004) 119–132.
[19] S. Libman, UPW quality and technology to support needs in advanced industries, Ultrapure Water J. (2014) 11–17.
[20] J. Degenova, F. Shadman, Recovery, reuse, and recycle of water in semiconductor wafer fabrication facilities, Environ. Prog. 16 (1997) 263–267.
[21] L. Diouri, W. Lei, W. Baoxu, X. Lijun, D. Xuebing, S. Choo, Control of severe membrane silica scaling: investigation and trouble shooting, Desalin. Water Treat. 55 (2015) 3471–3477.
[22] J. Drewes, G. Amy, M. Reinhard, Targeting bulk and trace organics during advanced membrane treatment leading to indirect potable reuse, 2002 Water Sources Conference: Reuse, Resources, Conservation, 2002, p. 18.
[23] J.E. Drewes, M. Reinhard, P. Fox, Comparing microfiltration-reverse osmosis and soil-aquifer treatment for indirect potable reuse of water, Water Res. 37 (2003) 3612–3621.
[24] G.D.G.C. John Wammes, J.R. Cooper, Enhanced TOC reduction in pharmaceutical water systems using highly reflective UV disinfection reactors, Ultrapure Water J. (2015) 11–16.
[25] ASTM, D4189-07 Standard Test Method for Silt Density Index (SDI) of Water ASTM Internailtional, West Conshohocken, (2014), pp. 1–3.
[26] ASTM, D8002-15 Standard Test Method for Modified Fouling Index (MFI) of Water, (2015), pp. 1–3.
[27] J.H. Kim, J.-Y. Hwang, H.R. Hwang, H.S. Kim, J.H. Lee, J.-W. Seo, U.S. Shin, S.-H. Lee, Simple and cost-effective method of highly conductive and elastic carbon nanotube/polydimethylsiloxane composite for wearable electronics, Sci. Rep. 8 (2018) 1375.
[28] ASTM, D5127-99 Standard Guide for Ultra-pure Water Used in the Electronics and Semiconductor Industries, American Society for Testing and Materials, USA, 1999, pp. 1–6.
[29] M.K.S.F.E. Boerlage, Z. Tarawneh, R. De Faber, J.C. Schippers, Development of the MFI-UF in constant flux filtration, Desalination 161 (2004) 103–113.
[30] S.G.S. Rodríguez, B. Al-Rabaani, M.D. Kennedy, G.L. Amy, J.C. Schippers, MFI-UF constant pressure at high ionic strength conditions, Desalin. Water Treat. 10 (2009).
[31] S.G. Salinas Rodríguez, Particulate and Organic Matter Fouling of SWRO Systems: Characterization, Modelling and Applications, CRS Press/Balkema, CRS Press/Balkema, 2011, pp. 1–254.
[32] S.F. Boerlage, M.D. Kennedy, M.R. Dickson, D.E. El-Hodali, J.C. Schippers, The modified fouling index using ultrafiltration membranes (MFI-UF): characterisation, filtration mechanisms and proposed reference membrane, J. Membr. Sci. 197 (2002) 1–21.
[33] S.G. Salinas-Rodriguez, G.L. Amy, J.C. Schippers, M.D. Kennedy, The modified fouling index ultrafiltration constant flux for assessing particulate/colloidal fouling of RO systems, Desalination 365 (2015) 79–91.
[34] J.-S. Choi, T.-M. Hwang, S. Lee, S. Hong, A systematic approach to determine the fouling index for a RO/NF membrane process, Desalination 238 (2009) 117–127.
[35] Z. Wang, J. Chu, X. Zhang, Study of a cake model during stirred dead-end microfiltration, Desalination 217 (2007) 127–138.
[36] J.M. Berg, A. Romoser, N. Banerjee, R. Zebda, C.M. Sayes, The relationship between pH and zeta potential of ~30 nm metal oxide nanoparticle suspensions relevant to in vitro toxicological evaluations, Nanotoxicology 3 (2009) 276–283.
[37] C. Zhou, Y. Bashirzadeh, T.A. Bernadowski, X. Zhang, UV light–induced aggregation of titania submicron particles, Micromachines 7 (2016) 203.
[38] J. Schippers, J. Verdouw, The modified fouling index, a method of determining the fouling characteristics of water, Desalination 32 (1980) 137–148.
[39] A.F. von Recum, Handbook of Biomaterials Evaluation: Scientific, Technical and Clinical Testing of Implant Materials, CRC Press, 1998.
[40] W. Han, W. Zhu, P. Zhang, Y. Zhang, L. Li, Photocatalytic degradation of phenols in aqueous solution under irradiation of 254 and 185 nm UV light, Catal. Today 90 (2004) 319–324.
[41] Z. Li, J.K. Muiruri, W. Thitsartarn, X. Zhang, B.H. Tan, C. He, Biodegradable silica rubber core-shell nanoparticles and their stereocomplex for efficient PLA toughening, Compos. Sci. Technol. 159 (2018) 11–17.
[42] S. Hong, R.S. Faibish, M. Elimelech, Kinetics of permeate flux decline in crossflow membrane filtration of colloidal suspensions, J. Colloid Interface Sci. 196 (1997) 267–277.
[43] Y. Ju, S. Hong, Nano-colloidal fouling mechanisms in seawater reverse osmosis process evaluated by cake resistance simulator-modified fouling index nanofiltration, Desalination 343 (2014) 88–96.

Abbreviations

CE: cellulose acetate
FDR: flux decline rate
IPA: isopropanol alcohol
LP: low pressure lamp
LMW: low molecular weight
MF: microfiltration
MFI: modified fouling index (s/L^2)
$MFI_{0.45}$: modified fouling index using a 0.45 μm membrane filter (s/L^2)
MFI-UF: modified fouling index ultrafiltration (s/L^2)
$MFI\text{-}UF_{flux}$: modified fouling index measured under constant flux condition (s/L^2)
$MFI\text{-}UF_{pres}$: modified fouling index measured under constant pressure condition (s/L^2)
MP: medium pressure lamp
RO: reverse osmosis
SAXS: small angle X-ray scattering
SDI: Silt Density Index (%/min)
TMP: transmembrane pressure (Pa)
TOC: total organic matter (ppm)
UPW: ultrapure water
UV: ultraviolet